Generating high-performance polarization measurements with low-performance polarizers: demonstration with a microgrid polarization camera

Nathan Hagen,[a,*] Shibata Shuhei,[a,b] and Yukitoshi Otani[a,b]
[a]Utsunomiya University, Center for Optical Research and Engineering, Department of Optical Engineering, Utsunomiya, Tochigi, Japan
[b]Utsunomiya University, Graduate School of Engineering, Utsunomiya, Tochigi, Japan

Abstract. Microgrid polarization cameras have historically experienced lower performance than is typical for monolithic polarization systems. Specifically, their polarizer elements have had a lower extinction ratio and a larger orientation error. We show how to use the calibrated parameters of a nonideal polarizer to modify the polarization measurement model, effectively allowing one to generate high-performance measurements from low-performance elements. We demonstrate the effectiveness of this approach on a commercial polarization camera and estimate the signal-to-noise ratio penalty for using nonideal polarizers in this camera as being 1.25× versus a system using ideal polarizers. [DOI: 10.1117/1.OE.58.8.080501]

Keywords: polarization; imaging polarimetry; noise.

Paper 190765L received Jun. 3, 2019; accepted for publication Aug. 5, 2019; published online Aug. 21, 2019.

A polarizer can be used to estimate the orientation and degree of linear polarization of light by rotating the polarizer to the four angles: 0 deg, 45 deg, 90 deg, and 135 deg and measuring the light intensity transmitted at each angle. In a polarization camera, this can be done in a single snapshot by combining the measurements of four adjacent pixels, each of which have micropolarizers oriented at each of the four orientation angles (Fig. 1).[1] For incoherent light, we can use the Stokes vector $\mathbf{s} = (s_0, s_1, s_2, s_3)^T$ to represent the input polarization state and the Mueller calculus to model the four intensities I_θ measured at the detector:

$$\begin{aligned} I_0 &= \frac{1}{2}(s_0 + s_1) + n_0, \\ I_{45} &= \frac{1}{2}(s_0 + s_2) + n_{45}, \\ I_{90} &= \frac{1}{2}(s_0 - s_1) + n_{90}, \\ I_{135} &= \frac{1}{2}(s_0 - s_2) + n_{135}, \end{aligned} \tag{1}$$

for random noise values n_θ. In the analysis to follow, we will assume all of the noise terms to have zero mean, i.e., $\langle I_i + n_i \rangle = I_i$ and $\langle n_i \rangle = 0$. This causes no difficulties for Poisson-distributed noise, since our definition of the signal I and noise n results in the mean value of the Poisson-distributed variable to be incorporated into I while n retains the zero-mean stochastic portion.

The four equations of (1) have the matrix form

$$\underbrace{\begin{pmatrix} I_0 \\ I_{45} \\ I_{90} \\ I_{135} \end{pmatrix}}_{\mathbf{I}} = \underbrace{\frac{1}{2}\begin{pmatrix} 1 & 1 & 0 & 0 \\ 1 & 0 & 1 & 0 \\ 1 & -1 & 0 & 0 \\ 1 & 0 & -1 & 0 \end{pmatrix}}_{\mathbf{W}} \underbrace{\begin{pmatrix} s_0 \\ s_1 \\ s_2 \\ s_3 \end{pmatrix}}_{\mathbf{s}} + \underbrace{\begin{pmatrix} n_0 \\ n_{45} \\ n_{90} \\ n_{135} \end{pmatrix}}_{\mathbf{n}} \tag{2}$$

or $\mathbf{I} = \mathbf{W}\mathbf{s} + \mathbf{n}$, where $\mathbf{W}$ is the measurement matrix. By inspection, we can obtain the input linear Stokes vector elements as

$$\begin{aligned} \hat{s}_0 &= \frac{1}{2}(I_0 + I_{45} + I_{90} + I_{135}), \\ \hat{s}_1 &= I_0 - I_{90}, \\ \hat{s}_2 &= I_{45} - I_{135}, \end{aligned} \tag{3}$$

or

$$\underbrace{\begin{pmatrix} \hat{s}_0 \\ \hat{s}_1 \\ \hat{s}_2 \end{pmatrix}}_{\hat{\mathbf{s}}} = \underbrace{\frac{1}{2}\begin{pmatrix} 1 & 1 & 1 & 1 \\ 2 & 0 & -2 & 0 \\ 0 & 2 & 0 & -2 \end{pmatrix}}_{\mathbf{A}} \underbrace{\begin{pmatrix} I_0 \\ I_{45} \\ I_{90} \\ I_{135} \end{pmatrix}}_{\mathbf{I}}, \tag{4}$$

i.e., $\mathbf{s} = \mathbf{A}\mathbf{I}$, where $\mathbf{A}$ is the analysis matrix. To evaluate the performance of a polarization measurement, we can use the measurement and analysis matrix elements to calculate the Stokes vector covariance matrix $\mathbf{K}$ as[2,3]

$$K_{ij} = \underbrace{\left[\sum_{k=0}^{3} s_k \sum_{\ell=0}^{3} A_{i\ell} A_{j\ell} W_{\ell k}\right]}_{\text{Poisson noise part}} + \underbrace{\left[v_\mathrm{d} \sum_{\ell=0}^{3} A_{i\ell} A_{j\ell}\right]}_{\text{Gaussian noise part}}, \tag{5}$$

where s_k is the k'th Stokes vector element in units of photoelectrons and v_d is the detector noise variance, also in units of photoelectrons. For an ideal polarizer, this set of four measurements produces variances in the Stokes vector components as[3]

*Address all correspondence to Nathan Hagen, E-mail: nh@hagenlab.org

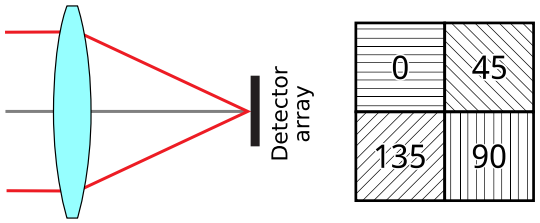

Fig. 1 A polarization camera showing a 2×2 pixels group from the detector array and their polarization filter orientations.

$$\begin{aligned}\mathrm{var}(\hat{s}_0) &= \frac{1}{2}s_0 + v_\mathrm{d},\\ \mathrm{var}(\hat{s}_1) &= s_0 + 2v_\mathrm{d},\\ \mathrm{var}(\hat{s}_2) &= s_0 + 2v_\mathrm{d}.\end{aligned} \tag{6}$$

The equally weighted variance (EWV) is often used to summarize the measurement performance, such that in this case EWV $= \frac{5}{2}s_0 + 5v_\mathrm{d}$.[3]

A nonideal linear polarizer is a diattenuator defined by its diattenuation D, its orientation α, and its efficiency η (the average transmission of the diattenuator for all input polarization angles):[4]

$$\mathbf{M}_\mathrm{ld} = \eta\begin{pmatrix} 1 & Dc & Ds & 0\\ Dc & 1-Ds^2 & \frac{1}{2\eta}Dcs & 0\\ Ds & \frac{1}{2\eta}Dcs & 1-Dc^2 & 0\\ 0 & 0 & 0 & 1-D\end{pmatrix}, \tag{7}$$

for $c = \cos(2\alpha)$ and $s = \sin(2\alpha)$. An ideal polarizer has $D = 1$, $\eta = 1$, and orientation α. The polarizer's extinction ratio X is derived from the diattenuation as $X = (1+D)/(1-D)$.

Modeling each pixel of a polarization camera as a nonideal polarizer, we can calibrate the diattenuation D_n and orientation α_n parameters at each pixel n, then use the Mueller calculus to estimate the polarization state by combining measurements I_i from each set of four neighboring pixels. This produces the measurement model[5]

$$\underbrace{\begin{pmatrix} I_0\\ I_2\\ I_3\\ I_4\end{pmatrix}}_{\mathbf{I}} = \underbrace{\frac{1}{2}\begin{pmatrix} 1 & D_0\cos(2\alpha_0) & D_0\sin(2\alpha_0)\\ 1 & D_1\cos(2\alpha_1) & D_1\sin(2\alpha_1)\\ 1 & D_2\cos(2\alpha_2) & D_2\sin(2\alpha_2)\\ 1 & D_3\cos(2\alpha_3) & D_3\sin(2\alpha_3)\end{pmatrix}}_{\mathbf{W}}\underbrace{\begin{pmatrix} s_0\\ s_1\\ s_2\end{pmatrix}}_{\mathbf{s}}. \tag{8}$$

The polarizer efficiency η does not appear here because it typically cannot be separated from the pixel's internal quantum efficiency q_int—the two appear together as the single factor $q_\mathrm{ext} = \eta q_\mathrm{int}$ as the "external" quantum efficiency. Because we do not calibrate the camera's quantum efficiency here, the equations below assume $q_\mathrm{ext} = 1$, so that the Stokes parameters are represented in units of photoelectrons rather than photons.

The general analytical form of $\mathbf{A}$ is quite complex, but if we assume that the orientation errors are small then we can use a Taylor expansion about their nominal values:

$$\begin{aligned}\cos(2\alpha_0) &= \cos(2\epsilon_0) \to 1,\\ \cos(2\alpha_1) &= \cos(90^\circ + 2\epsilon_1) \to -2\epsilon_1,\\ \cos(2\alpha_2) &= \cos(180^\circ + 2\epsilon_2) \to -1,\\ \cos(2\alpha_3) &= \cos(270^\circ + 2\epsilon_3) \to 2\epsilon_3,\end{aligned}$$

and

$$\begin{aligned}\sin(2\alpha_0) &= \sin(2\epsilon_0) \to 2\epsilon_0,\\ \sin(2\alpha_1) &= \sin(90^\circ + 2\epsilon_1) \to 1,\\ \sin(2\alpha_2) &= \sin(180^\circ + 2\epsilon_2) \to -2\epsilon_2,\\ \sin(2\alpha_3) &= \sin(270^\circ + 2\epsilon_3) \to -1,\end{aligned}$$

where ϵ_n represents the angular error about the nominal orientation. Likewise, each diattenuation can be represented as $D_i = 1 - \Delta_i$, where the diattenuation errors Δ_i are assumed to be small. For this first-order approximation regime, the analysis matrix $\mathbf{A}$ in the Stokes vector estimation:

$$\underbrace{\begin{pmatrix} \hat{s}_0'\\ \hat{s}_1'\\ \hat{s}_2'\end{pmatrix}}_{\hat{\mathbf{s}}'} = \underbrace{\frac{1}{4}\begin{pmatrix} A_{00} & A_{01} & A_{02} & A_{03}\\ A_{10} & A_{11} & A_{12} & A_{13}\\ A_{20} & A_{21} & A_{22} & A_{23}\end{pmatrix}}_{\mathbf{A}}\underbrace{\begin{pmatrix} I_0\\ I_1\\ I_2\\ I_3\end{pmatrix}}_{\mathbf{I}} \tag{9}$$

simplifies to

$$\begin{aligned}A_{00} &= 2 + \Delta_0 - \Delta_2 + 2\epsilon_1 - 2\epsilon_3,\\ A_{01} &= 2 + \Delta_1 - \Delta_3 - 2\epsilon_0 + 2\epsilon_2,\\ A_{02} &= 2 - \Delta_0 + \Delta_2 - 2\epsilon_1 + 2\epsilon_3,\\ A_{03} &= 2 - \Delta_1 + \Delta_3 + 2\epsilon_0 - 2\epsilon_2,\\ A_{10} &= 4 + \Delta_0 + 3\Delta_2 + 2\epsilon_1 - 2\epsilon_3,\\ A_{11} &= \Delta_0 - \Delta_2 - 4\epsilon_0 + 2\epsilon_1 + 4\epsilon_2 - 2\epsilon_3,\\ A_{12} &= -4 - 3\Delta_0 - \Delta_2 + 2\epsilon_1 - 2\epsilon_3,\\ A_{13} &= \Delta_0 - \Delta_2 + 4\epsilon_0 - 2\epsilon_1 + 4\epsilon_2 + 2\epsilon_3,\\ A_{20} &= \Delta_1 - \Delta_3 + 2\epsilon_0 + 4\epsilon_1 - 2\epsilon_2 + 4\epsilon_3,\\ A_{21} &= 4 + \Delta_1 + 3\Delta_3 - 2\epsilon_0 + 2\epsilon_2\\ A_{22} &= \Delta_1 - \Delta_3 + 2\epsilon_0 - 4\epsilon_1 - 2\epsilon_2 - 4\epsilon_3,\\ A_{23} &= -4 - 3\Delta_1 - \Delta_3 - 2\epsilon_0 + 2\epsilon_2.\end{aligned} \tag{10}$$

Here, $\hat{s}_1'$ indicates the calibration-corrected Stokes estimate, while $\hat{s}_i$ without a prime indicates the estimate assuming an ideal polarizer. In Eqs. (9) and (10), note that it is generally not useful to define α_0 as anything but zero, since the system reference axis is a degree of freedom that we have to choose in most situations. In this case, we can set $\epsilon_0 = 0$.

To demonstrate this technique, we use a commercially available polarization camera to measure the Stokes vector elements of the light transmitted through a high-extinction-ratio Glan–Thompson polarizer as the polarizer is rotated through a set of angles from 0 deg to 180 deg. The polarization camera is a photonic lattice PI-110, having

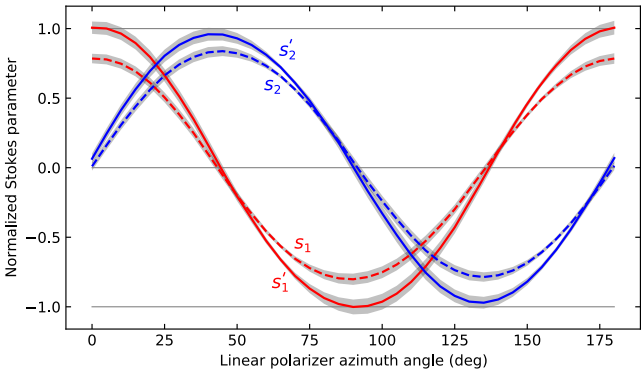

Fig. 2 The measured uncorrected linear Stokes parameters $\hat{s}_1$ and $\hat{s}_2$ and corrected parameters $\hat{s}_1'$ and $\hat{s}_2'$ obtained while rotating the input angle of polarization from 0 deg to 180 deg. Note that the Stokes parameters, here, are shown in their normalized form: $\tilde{s}_1 = s_1/s_0$ and $\tilde{s}_2 = s_2/s_0$. Each curve is obtained as an average of the results from all pixels of the camera, while the grayed regions astride each curve give the standard deviation of the result, also calculated using all pixels on the camera. The dashed curves indicate the measurement result using the ideal polarization analysis matrix [Eq. (4)] and the solid curves give the measurement with the corrected analysis matrix [Eq. (10)].

1164×874 pixels of 4.65-μm size, 20-Hz frame rate, 12-bit depth, and 520 ± 20-nm wavelength range. Figure 2 shows the resulting Stokes parameter estimates before ($\hat{s}_1$ and $\hat{s}_2$) and after ($\hat{s}_1'$ and $\hat{s}_2'$) applying the correction, corresponding to using the ideal polarization analysis matrix [Eq. (4)] or a corrected analysis matrix [Eq. (10)]. We can see that the corrected curves display a higher contrast than the uncorrected curves, so that the mean values of the Stokes parameter (averaged across all camera pixels) at each angle of the input polarizer are closer to the correct values. Looking closely at the curves, we can also see that the standard deviation of the corrected result is slightly larger than for the uncorrected measurement.

To see why the corrected result has higher noise, we can use Eqs. (5), (8), and (10) in their analytical form to calculate the general equation for the variances. To keep the expressions as simple as possible, and because our experimental data show that the diattenuation errors are much larger than the angular errors in our system, we set the angular errors to zero ($\epsilon_i \approx 0$). Thus, in the detector-limited noise regime (uniform Gaussian noise), the variances become

$$\begin{aligned}
\mathrm{var}(\hat{s}_0') &= \frac{v_\mathrm{d}}{8}[8 + \Delta_0^2 + \Delta_1^2 + \Delta_2^2 + \Delta_3^2 - 2\Delta_0\Delta_2 - 2\Delta_1\Delta_3] \\
&\approx v_\mathrm{d}, \\
\mathrm{var}(\hat{s}_1') &= \frac{v_\mathrm{d}}{4}[8 + 3\Delta_0^2 + 3\Delta_2^2 + 2\Delta_0(\Delta_2 + 4) + 8\Delta_2] \\
&\approx 2v_\mathrm{d}[1 + \Delta_0 + \Delta_2], \\
\mathrm{var}(\hat{s}_2') &= \frac{v_\mathrm{d}}{4}[8 + 3\Delta_1^2 + 3\Delta_3^2 + 2\Delta_1(\Delta_3 + 4) + 8\Delta_3] \\
&\approx 2v_\mathrm{d}[1 + \Delta_1 + \Delta_3],
\end{aligned} \tag{11}$$

where the variances are the diagonal elements of the Stokes vector covariance matrix, $\mathrm{var}(\hat{s}_0') = K_{00}$, etc. The approximations in Eq. (11) assume small errors so that only the first-order terms are retained. In this approximation, $\mathrm{var}(\hat{s}_0')$ is independent of the diattenuation errors Δ_i, while $\mathrm{var}(\hat{s}_1')$ increases linearly with Δ_0 and Δ_2, and $\mathrm{var}(\hat{s}_2')$ with Δ_1 and Δ_3, respectively. The Stokes parameters are often expressed in normalized form $\tilde{s}_i = s_i/s_0$, for which the expressions in (11) need to be modified. The normalized parameter variances are related to their unnormalized counterparts by[6]

$$\mathrm{var}(\tilde{s}_i') = \frac{1}{\langle s_0' \rangle^2}\,\mathrm{var}(s_i') + \frac{\langle s_i' \rangle^2}{\langle s_0' \rangle^4}\mathrm{var}(s_0'), \tag{12}$$

which together with Eq. (11) gives

$$\begin{aligned}
\mathrm{var}(\tilde{s}_1') &= \frac{v_\mathrm{d}}{s_0^2}(2[1 + \Delta_0 + \Delta_2] + \tilde{s}_1^2), \\
\mathrm{var}(\tilde{s}_2') &= \frac{v_\mathrm{d}}{s_0^2}(2[1 + \Delta_1 + \Delta_3] + \tilde{s}_2^2),
\end{aligned} \tag{13}$$

and where we have replaced the corrected parameter means with the true parameter values: $\langle s_0' \rangle \to s_0$, etc.

To see how these variance equations behave quantitatively, we can look at an example group of 4 pixels on the polarization camera. For this group, we obtain calibrated diattenuations of

$$D_0 = 0.8277, \quad D_1 = 0.7435, \quad D_2 = 0.8133, \quad D_3 = 0.7338,$$

and calibrated orientation angles of

$$\begin{aligned}
\alpha_0 &= 0 \ \text{deg}, \quad \alpha_1 = 49.650 \ \text{deg}, \\
\alpha_2 &= 88.694 \ \text{deg}, \quad \alpha_3 = 134.399 \ \text{deg},
\end{aligned}$$

so that the differences from the nominal angles are 0 deg, 4.650 deg, −1.306 deg, and −0.601 deg. Converting the angular errors to radians for the ϵ_i values, we obtain the error parameters:

$$\begin{aligned}
&\Delta_0 = 0.1723, \quad \Delta_1 = 0.2565, \quad \Delta_2 = 0.1867, \quad \Delta_3 = 0.2662, \\
&\epsilon_0 = 0, \quad \epsilon_1 = 0.0811, \quad \epsilon_2 = -0.0228, \quad \epsilon_3 = -0.0105.
\end{aligned} \tag{14}$$

With these parameters, the variances (11) in the detector-limited noise regime (uniform Gaussian noise) become, via Eq. (5),

$$\mathrm{var}(\hat{s}_0') = 1.00v_\mathrm{d}, \quad \mathrm{var}(\hat{s}_1') = 3.23v_\mathrm{d}, \quad \mathrm{var}(\hat{s}_2') = 3.01v_\mathrm{d}, \tag{15}$$

for detector noise variance v_d. In comparison to Eq. (6), we see that the corrected nonideal measurement for this pixel group suffers an increase in the variances for measuring s_1 and s_2 by factors of 1.62 and 1.51, respectively, while the variance for s_0 is basically unaffected. These correspond to a loss in signal-to-noise ratio (SNR) by factors of 1.27 in s_1 and 1.23 in s_2.

Using the same Eqs. (2), (5), and (10), we can obtain similar results for the Poisson noise regime, for which the variance equations become

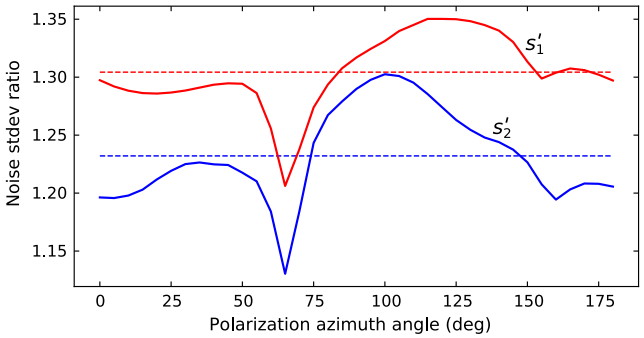

Fig. 3 The increase (multiplying factor) in the normalized Stokes parameter standard deviations std($\hat{s}_1'$) and std($\hat{s}_2'$) with respect to the input polarization angle, where the increased noise is caused by applying the correction of Eq. (9). The dashed lines indicate the average standard deviation ratio taken across all angles.

$$\begin{aligned}
\mathrm{var}(\hat{s}_0') &\approx \frac{1}{2}s_0 + \frac{1}{8}s_1(\Delta_0 - \Delta_2) + \frac{1}{8}s_2(\Delta_1 - \Delta_3),\\
\mathrm{var}(\hat{s}_1') &\approx s_0(1 + \Delta_0 + \Delta_2) + s_1(\Delta_2 - \Delta_0),\\
\mathrm{var}(\hat{s}_2') &\approx s_0(1 + \Delta_1 + \Delta_3) + s_2(\Delta_3 - \Delta_1),
\end{aligned} \tag{16}$$

where only the first-order terms are retained. As we expect, the variances of Eqs. (11) and (16) approach those of the ideal polarizer system[3] as the diattenuation errors approach zero ($\Delta_i \to 0$).

For mixed Gaussian–Poisson noise, the Gaussian and Poisson expressions (11) and (16) are simply added together to get the total variance. Using the example diattenuation errors of Eq. (14), the Stokes parameter variances under Poisson noise become

$$\begin{aligned}
\mathrm{var}(\hat{s}_0') &= 0.500s_0 - 0.001s_1 - 0.002s_2,\\
\mathrm{var}(\hat{s}_1') &= 1.542s_0 + 0.092s_1 + 0s_2,\\
\mathrm{var}(\hat{s}_2') &= 1.381s_0 + 0s_1 + 0.014s_2.
\end{aligned} \tag{17}$$

The results of Eqs. (15) and (17) and Fig. 3 demonstrate an SNR penalty due to reduced diattenuation that is similar to that calculated by Tyo and Wei,[7] where the authors concluded via numerical simulation that polarizer extinction ratios as low as 3 give a 3.5 dB (i.e., a factor of 2.2) penalty in SNR. Although the measurement system analyzed by Tyo and Wei is not the same as the one we consider, here, the SNR penalty is similar in magnitude. Our results also agree with those of Roussel et al.,[8] who analyzed microgrid polarization cameras and concluded that diattenuations of 0.75 to 0.85 will increase the variance in the estimated degree of polarization by 1.6 to 3. What is different from Roussel et al. is that the analytic dependence of the Stokes parameter variance is expressed here in terms of the calibration parameters directly, allowing us to see more clearly the effect of misalignment or low diattenuation on the measurements.

In Fig. 2, we can see that the mean values of the corrected curves come close to the ideal behavior of a cosine curve oscillating between $+1$ and -1. The shaded regions surrounding each curve describe the values within one standard deviation about the mean, where we can expect to find the data most of the time. The noise fluctuations result primarily from the shot noise of the measurements, but are also influenced by any error in the calibration parameters. As we can expect for any linear estimation procedure, as the estimate approaches the ideal cosine curve, noise fluctuations cause some of the data at the peaks and valleys to extend beyond the physically valid region between $+1$ and -1.

From these results, we can see that most polarimeters can tolerate a surprisingly low diattenuation if calibrated well. As often is the case for indirect measurements, it is the accuracy with which one can calibrate the system measurement model that limits the measurement performance more than the inherent accuracy of the components themselves. If we work with low-extinction-ratio polarizers, we can still achieve high-accuracy measurements, but only if we take extreme care in the calibration and in ensuring the accuracy of our reconstruction.[9] For example, we should keep in mind that the diattenuation value of a pixel is a spectrally dependent quantity, so that the measurement spectrum must be similar to the spectrum used during calibration in order for the results to be accurate.[10]

References

1. Y. Maruyama et al., "3.2-MP back-illuminated polarization image sensor with four-directional air-gap wire grid and 2.5-μm pixels," *IEEE Trans. Electron Devices* **65**, 2544–2551 (2018).
2. F. Goudail, "Optimization of the contrast in active Stokes images," *Opt. Lett.* **34**, 121–123 (2009).
3. N. Hagen and Y. Otani, "Stokes polarimeter performance: general noise model and analysis," *Appl. Opt.* **57**, 4283–4296 (2018).
4. R. A. Chipman, "Polarimetry," Chapter 22 in *Handbook of Optics*, M. Bass, Ed., Vol. **2**, 2nd ed., pp. 22.1–22.37, McGraw-Hill, New York (1995).
5. N. Hagen, S. Shibata, and Y. Otani, "Calibration and performance assessment of microgrid polarization cameras," *Opt. Eng.* **58**, 082408 (2019).
6. N. Hagen, "Statistics of normalized Stokes polarization parameters," *Appl. Opt.* **57**, 5356–5363 (2018).
7. J. S. Tyo and H. Wei, "Optimizing imaging polarimeters constructed with imperfect optics," *Appl. Opt.* **45**, 5497–5503 (2006).
8. S. Roussel, M. Boffety, and F. Goudail, "Polarimetric precision of a micropolarizer grid-based camera in the presence of additive and Poisson shot noise," *Opt. Express* **26**, 29968–29982 (2018).
9. J. S. Tyo, "Design of optimal polarimeters: maximization of signal-to-noise ratio and minimization of systematic error," *Appl. Opt.* **41**, 619–630 (2002).
10. N. Hagen, "Flatfield correction errors due to spectral mismatching," *Opt. Eng.* **53**(12), 123107 (2014).